CHEMISTRY
A EUROPEAN JOURNAL

DOI: 10.1002/chem.200901209

The Role of Transferrin in Actinide(IV) Uptake: Comparison with Iron(III)

Aurélie Jeanson,[a, b] M. Ferrand,[c] Harald Funke,[d] Christoph Hennig,[d] Philippe Moisy,[a] Pier Lorenzo Solari,[e] Claude Vidaud,[f] and Christophe Den Auwer*[a]

Abstract: The impact of actinides on living organisms has been the subject of numerous studies since the 1950s. From a general point of view, these studies show that actinides are chemical poisons as well as radiological hazards. Actinides in plasma are assumed to be mainly complexed to transferrin, the iron carrier protein. This paper casts light on the uptake of actinides(IV) (thorium, neptunium, plutonium) by transferrin, focusing on the pH dependence of the interaction and on a molecular description of the cation binding site in the protein. Their behavior is compared with that of iron(III), the endogenous transferrin cation, from a structural point of view. Complementary spectroscopic techniques (UV/Vis spectrophotometry, microfiltration coupled with γ spectrometry, and X-ray absorption fine structure) have been combined in order to propose a structural model for the actinide-binding site in transferrin. Comparison of our results with data available on holotransferrin suggests some similarities between the behavior of Fe^{III} and $Np^{IV}/Pu^{IV}/ Np^{IV}$ is not complexed at pH <7, whereas at pH ≈ 7.4 complexation can be regarded as quantitative. This pH effect is consistent with the in vivo transferrin "cycle". Pu^{IV} also appears to be quantitatively bound by apotransferrin at around pH ~7.5, whereas Th^{IV} was never complexed under our experimental conditions. EXAFS data at the actinide edge have allowed a structural model of the actinide binding site to be elaborated: at least one tyrosine residue could participate in the actinide coordination sphere (two for iron), forming a mixed hydroxo–transferrin complex in which actinides are bound with transferrin both through An–tyrosine and through An−OH bonds. A description of interatomic distances is provided.

Keywords: actinides · EXAFS spectroscopy · neptunium · plutonium · transferrin

Introduction

Internal contamination of living organisms with actinides (Th, U, Np, Pu, Am) under either acute or chronic conditions has the potential to induce both radiological and chemical toxicity. Whatever the means of contamination (inhalation, ingestion, or wound), the radionuclide is absorbed into, and then transported by, blood before being deposited in the target organs in which it is stored and then slowly eliminated in the urine and feces.

The impact of actinides on living organisms has been studied in depth since the 1950s. These studies show that actinides are both chemical poisons and radiological hazards. Because of their strong tendency to undergo hydrolysis at physiological pH values, actinide ions in living organisms can only exist in complexed form or as hydrolyzed species.[1] Once they are solubilized and transported into the blood, deposition and excretion of the absorbed actinides are essentially independent of their route of entry. Liver is the most important soft tissue deposition site for all the actinides except uranyl, in which case it is the kidneys. The skel-

[a] Dr. A. Jeanson, Dr. P. Moisy, Dr. C. Den Auwer
CEA, Nuclear Energy Division
Radiochemistry Process Department, SCPS/LILA
30207 Bagnols sur Cèze (France)
Fax: (+33) 466796325
E-mail: christophe.denauwer@cea.fr

[b] Dr. A. Jeanson
Now at SUBATECH, Ecole des Mines de Nantes
44307 Nantes (France)

[c] Dr. M. Ferrand
CEA Grenoble DSV/iRTSV/DIR, 38054 Grenoble (France)

[d] Dr. H. Funke, Dr. C. Hennig
Forschungszentrum Dresden-Rossendorf
Institute of Radiochemistry, 01314 Dresden (Germany)

[e] Dr. P. L. Solari
Synchrotron SOLEIL, MARS beam line
91192 Gif sur Yvette (France)

[f] Dr. C. Vidaud
CEA Marcoule DSV/iBEB/SBTN
30207 Bagnols sur Cèze (France)

eton is also a major deposition site for the actinides in all of the oxidation states that have been administered to animals.[2] In a review by Taylor concerning actinide speciation in blood,[1] it is shown that most of the total U and Th found in blood is associated with the blood cells, whereas 90% of the Pu^{IV}, Am^{III}, Cm^{III}, or Cf^{III} in blood is found in plasma. Moreover, actinides in plasma are assumed to be mainly complexed to transferrin (Tf), the iron carrier protein.[1] A summarized review of the interaction of actinides with biomolecules has been published elsewhere.[3]

Transferrins are monomeric glycoproteins of about 80 kDa, used for the solubilization, sequestration, and transport of ferric iron. Three main families of transferrins are known: serum transferrin, which represents 3% of plasmatic proteins, lactoferrin, present in secretory fluids, and ovotransferrin, the protein of avian egg white.[4] The single polypeptide chain of 670–700 amino acids is folded into two globular lobes joined by a short connecting polypeptide. The two lobes, constituting the N-terminal and C-terminal halves of the molecule, each contain a single iron-binding site and have essentially the same folding. However, iron affinity seems to be slightly higher for the C-terminal lobe than for the N-terminal one.[5]

Each lobe is composed of two separately folded domains, which gives the protein great flexibility. When Fe^{III} is complexed the transferrin lobes are closed and the two domains draw nearer. The cellular transferrin receptors in target organs selectively bind holotransferrin, in which both lobes are closed, to the detriment of apotransferrin, which is fully open.[4,6] The holotransferrin form is then internalized through endocytosis. A proton pump decreases the pH inside the vesicle, causing the opening of the transferrin lobes, which release their iron cations inside the cell. The protein is then liberated and reenters circulation in its free form (apotransferrin).

Several holotransferrin structures have been determined by X-ray diffraction. The iron ligands in each lobe are two tyrosine phenolate oxygen atoms, one histidine imidazole nitrogen atom, and one carboxylic oxygen atom from an aspartate residue. A synergistic anion is also required for complexation, to form a distorted octahedron coordination sphere. In physiological media, carbonate, in its bidentate coordination mode, plays the role of synergistic anion. Under carbonate-free conditions, however, some other organic anions, such as oxalate, lactate, or nitrilotriacetate, can also play this role.[4,7]

Pu^{IV} and Fe^{III} display many similarities in their chemical and biological transport properties, as well as in their distributions.[8] Similarities such as ionic potential (z/r) for Fe^{III} and Pu^{IV} (4.6 and 4.2 e $Å^{-1}$, respectively), formation of highly insoluble hydroxides, and similar first hydrolysis constants [$Pu(OH)^{3+}$ and $Fe(OH)^{2+}$], to give just a few examples, may represent some key parameters. Similarities in the chemical behavior of Pu^{IV} and Fe^{III} have also been observed in protein systems such as the transferrin one. Indeed, Pu^{IV} has been reported bound to transferrin in the iron site location.[9,10] Homology is also to be expected for Np^{IV} and Th^{IV}, which are chemically relatively similar to Pu^{IV}. According to Durbin,[2] all the actinides investigated form variably stable complexes with plasma transferrin, in the following order:

$$Pu^{IV} > Th^{IV} > Np^{IV} \gg U^{VI}O_2^{2+} > Cf^{III} > Am^{III} > Cm^{III} \quad (a)$$

$Np^{V}O_2^{+}$ is only weakly complexed.[11] These actinide complexes are less stable than Fe–Tf, and the actinides are displaced from transferrin on addition of Fe^{III} to the reaction medium.[2,12–15] Similarly to Fe–Tf, the Pu^{IV}-, Th^{IV}-, and uranyl–Tf complexes are pH dependent, and begin to dissociate at pH <7.[16] The actinides that form the most stable transferrin complexes are cleared from the bloodstream slowly, whereas those that form weak complexes are cleared at much faster rates.[2] Harris et al.[17] report that at physiological pH, transferrin may bind two thorium ions at nonequivalent sites. In this assumption, the C-terminal binding site of transferrin coordinates through two tyrosine residues but the N-terminal site only through one. Apotransferrin has also been shown by numerous methods[18–21] to bind two uranyl ions, at the apotransferrin iron-binding sites. A binding mode involving two tyrosines and at least one carboxylate oxygen in the equatorial plane has been proposed. The oxo oxygen atoms seem to prevent the histidine at the iron complexation site from binding the uranium cation. The study also points out that the binding domains remain in a partially open conformation upon binding of UO_2^{2+}.[18] Complexation of Np^{IV} with transferrin and NTA (nitrilotriacetic acid) as a synergistic anion has already been investigated by Racine[11] and by Llorens et al.[22] The uptake of two Np^{IV} ions in the presence of the synergistic anion was suggested. Complexation of Np^{IV} with transferrin is characterized in the visible region by the appearance of bands at 747, 732, and 727 nm while the band at 740 nm decreases. A preliminary EXAFS study of the Np–Tf complex has shown that the actinide is mostly bound to the protein through oxygen and/or nitrogen donor functions, with a coordination number of around eight, which may include water molecules.[22,23] Complexation of plutonium(IV) with transferrin has also been confirmed.[9,10,24] Indeed, Duffield et al. found that the binding of plutonium involved the same binding sites as those used for iron,[24] although UV difference spectra are equivocal.[4,25] However, in vitro studies have shown that Pu^{IV} apparently does not induce the closure of the transferrin lobes,[26] and $Pu^{IV}{}_2$–Tf was not recognized by transferrin membrane receptors in liver cells.[10,11,27]

Although there is a tremendous volume of data available on the interaction of plutonium (and to lesser extents neptunium and thorium) with living organisms, nearly all of these studies are limited to macroscopic or physiological measurements, with no specific information at the molecular level. Molecular approaches have been undertaken more rarely, due to the combined intricacy of metallobiochemistry and actinide chemistry. However, such "molecular speciation" in actinide biomolecules is of considerable interest for understanding of the potential transport of radionuclides inside

living organisms. The interactions of actinides with various cells and tissue constituents are important not only for better understanding of the mechanisms governing their specific tissue deposition patterns and the initiation of toxic effects, but also for their important input in providing guidance on the structures, affinities, and design of potential specific chelating agents that might be used to eliminate an incorporated radionuclide.

This paper reports new insights into the uptake of actinides(IV) by transferrin, focusing on the pH dependence of the interactions and on a molecular description of the complexes formed. The behavior of Th, Np, and Pu is compared with that of iron(III), the transferrin endogenous cation, from a structural point of view. From the perspective of fundamental actinide molecular chemistry, it also addresses the question of fine-tuning of the cations' chemical properties across the series when dealing with very intricate ligands, because transferrin may be considered in terms of a simplistic approximation.

Results

Underlining neptunium complexation—UV/Visible/NIR spectrophotometry: As a first step, we chose UV/Vis/NIR spectrophotometry to identify the existence of an An^{IV}–Tf complex. This study was undertaken with Np^{IV}, because thorium(IV) does not show any electronic transitions in this energy range and plutonium(IV) signals are masked by transferrin signals, its molar extinction constant being very small in relation to that of transferrin ($\varepsilon_{Pu,\lambda=476} = 56\ L\,cm^{-1}\,mol^{-1}$; $\varepsilon_{Tf,\lambda=279} = 93\,000\ L\,cm^{-1}\,mol^{-1}$). Figure 1a shows the 650–800 nm range of the absorption spectrum of $[Np^{IV}(nta)_2]$ at pH 7.4, followed by addition of increasing amounts of transferrin. Upon addition, the absorption bands at 741 nm and 978 nm—characteristic of $[Np^{IV}(nta)_2]$ species[37]—decrease, while new peaks appear at 747, 733, and 995 nm. This evolution is characteristic of the formation of the Np–NTA–Tf complex.[23] Spectrophotometric titration of an $[Np^{IV}(nta)_2]$ solution in the presence of transferrin (0.5 equiv) as a function of pH was also undertaken by gradual addition of LiOH (1 M). Figure 1b shows the evolution of the absorption band at 741 nm with pH values between 6.1 and 8.6. From pH 6.1 to 6.9, no variation in the signal was observed, meaning that within this pH range Np^{IV} stays in the $[Np^{IV}(nta)_2]$ form in the presence of transferrin. When the pH is increased from pH 7.1 the absorption band at 741 nm decreases, while a peak at 747 nm appears. Again, this evolution is characteristic of the formation of the Np–NTA–Tf complex.[23] The absence of any significant signal in the 400–650 nm region demonstrates that formation of hydrolyzed neptunium species is negligible within this pH range.[28] To confirm these results, we extended our measurements as far as pH 8.6 to achieve precipitation of the actinide hydroxides. For pH $\geq$8.5, traces of solids or colloids appeared (opalescent solution), probably due to the precipitation of hydrolysed products of Np^{IV}. Those results are consistent with Racine's studies:[11] neptunium(IV) complexation is significant at pH $\geq$7 and at its maximum at pH 8, above which precipitation of the hydroxide occurs.

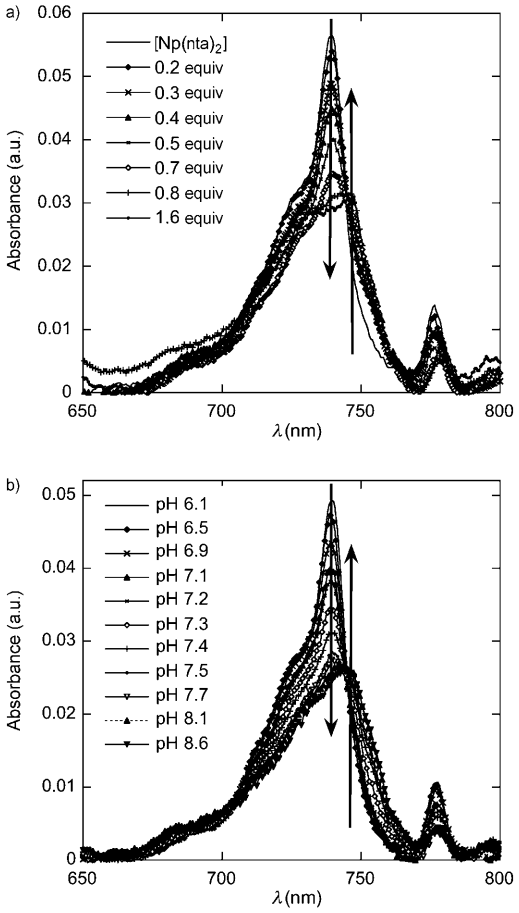

Figure 1. a) Titration of the $[Np(nta)_2]$ complex by increasing the stoichiometric amount of *apo*Tf from 0.1 to 1.6 equivalents (see Experimental Section and Table 2 for details). b) Titration of the Np–NTA–Tf complex by increasing proton concentration, from pH 6.1 to 8.6 (see Experimental Section and Table 1 for details).

Quantifying thorium and neptunium complexation—microfiltration and gamma spectrometry: In a second step, microfiltration followed by gamma spectrometry was undertaken for ^{232}Th and ^{237}Np to monitor the relative molar percentages of An^{IV} bound to transferrin as a function of pH for 5 $\leq$ pH $\leq$ 8. Quantification of ^{239}Pu complexation by this technique was not possible because the gammametric yield of this plutonium isotope is negligible and no other appropriate isotope was available. The fractions of An^{IV} in the filtrates relative to the initial quantities of $[An^{IV}(nta)_2]$ were monitored by gamma spectrometry as detailed in the Experimental Section. In order to validate the method for molecular weights smaller or larger than 10 kDa (i.e., in our case, 0% of Tf–An complex and 100% of Tf–An complex), two test experiments were carried out, the first one with $[Np^{IV}(nta)_2]$ complex in HEPES solution at pH 6 without transferrin, and the second one with *apo*Tf alone in HEPES solution at

pH 7.4. The gamma measurement of the first solution indicated that 90% of the actinide was present in the filtrate, showing that the molecular weight cut-off allows molecules smaller than 10 kDa to pass through. UV spectrophotometric measurement of the second solution was undertaken at 278 nm (this wavelength being characteristic of proteins). The spectrum indicated that 0.3% of the transferrin was present in the filtrate, showing that the molecular weight cut-off efficiently retains the protein on the filter. The molecular weight cut-off is thus efficient enough to ensure the separation of the An–NTA–Tf complex from $[An(nta)_2]$. One drawback of this technique is that separation of actinide–transferrin complexes from potential colloidal species (which according to Moriyama et al.[29] can have molecular weights higher than 100 kDa) is not possible. Figure 2 shows the evolution of the percentages of actinide not bound to transferrin as a function of pH for thorium and neptunium. For thorium, whatever the pH, almost all of the initial quantity of Th^{IV} was found in the filtrate, so these results suggested that, under our experimental conditions, Th^{IV} is not, or is only insignificantly, complexed to transferrin. Furthermore, under these conditions, at a pH of less than 8, thorium does not form high-molecular-weight hydrolysed products either.

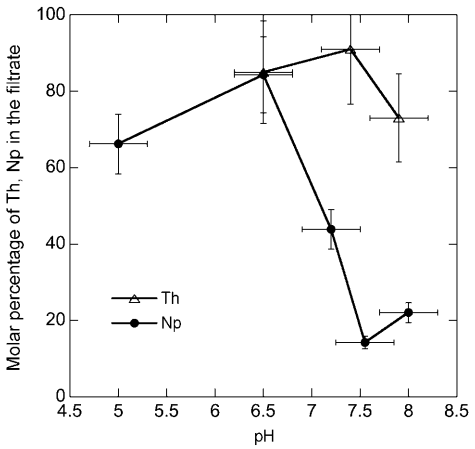

Figure 2. Comparative molar percentages of neptunium and thorium in the filtrates after centrifugation of Th–NTA–Tf and Np–NTA–Tf complexes as a function of pH. Gammametric measurements. See Experimental Section for details.

In contrast, the percentage of neptunium in the filtrate after centrifugation varied with pH. This result suggests that Np^{IV} uptake by transferrin is pH dependent: it was negligible for pH <7, reached a maximum for pH 7.5, and a plateau at pH ≥ 7.5, at which 80% of the Np^{IV} was bound to transferrin. These data are consistent with the spectrophotometric titration data.

Identification of the actinide coordination spheres—EXAFS: In a third step, and in order to investigate the structure of the actinide coordination spheres upon complexation by transferrin, an EXAFS study at the actinide L_{III} edges in An^{IV}–NTA–Tf ($An^{IV} = Th^{IV}$, Np^{IV}, Pu^{IV}) was undertaken. The evolution of the EXAFS oscillations as a function of pH was monitored in order to relate the local structural data to the spectrophotometric and microfiltration measurements described above.

Actinide L_{III} edge EXAFS spectra of An–NTA–Tf complexes (for Th: pH 5, 7.9; for Np: pH 5, 6, 6.5, 7.7, 8; for Pu: pH 6, 7.7, 8) were recorded and compared with the EXAFS spectra of $[An^{IV}(nta)_2]$, as shown in Figures 3a, 4a, and 5a. Corresponding Fourier transforms showing the pseudo radial distribution functions are presented in Figures 3b, 4b, and 5b. A qualitative comparison of the Th–NTA–Tf spectra with the EXAFS $[Th(nta)_2]$ spectrum unambiguously shows that whatever the pH of the medium, the EXAFS spectra remain unchanged (Figure 3a). This confirms the microfiltration/gammametric measurements suggesting that Th^{IV} is not complexed by transferrin under these conditions. Similarly, in the cases of Np^{IV} and Pu^{IV}, both actinide cations remain in the $[An(nta)_2]$ form at pH ≤ 6.5, and therefore do not bind to transferrin. When the pH values of the media were increased, evolution of the EXAFS spectra was clearly observed for Np–NTA–Tf and Pu–NTA–Tf at pH >7: a beating around 9.2 and 9.7 $Å^{-1}$, respectively, appears at pH 7.5. As a consequence, splitting of the first coordination shells of neptunium and plutonium is occurring on the pseudo radial distribution functions above pH 7.5. The evolution of the coordination spheres of Np^{IV} and Pu^{IV} is presumably due to complexation of both cations by transferrin, as suggested in the case of neptunium by the spectrophotometric and microfiltration measurements. The presence of the first short-range contribution at $R+\Phi = 1.8$ Å in the Fourier transform (FT
) precludes the presence of oxidized forms of Np or Pu (in neptunyl and plutonyl adducts the first oxo contribution typically occurs around $R+\Phi = 1.4$ Å). This was also confirmed by recording of the XANES L_{III} spectra of the two solutions (not shown). The absence of any shoulder at about 15 eV above the white line maximum that is well known to be the fingerprint of neptunyl and plutonyl adducts confirms that no oxidation of the cations had occurred.[30] This first qualitative interpretation sheds light on the competition between NTA and transferrin as a function of pH. It is also consistent with the spectrophotometric and microfiltration/gammametric results discussed above.

According to the above observations, the EXAFS spectra of An–NTA–Tf at pH <7.5 for $An = Np^{IV}$ and Pu^{IV}, and of Th–NTA–Tf at all pH values, were fitted in the same manner as for $[An^{IV}(nta)_2]$, as described elsewhere.[37] In this method, the entire coordination sphere of the actinide cation obtained from the model clusters is fitted as a semi-rigid polyhedron with only four structural parameters. This fitting method assumes that the coordination sphere of the complex element is similar to that of the model used. EXAFS parameters and model descriptions for the $[An(nta)_2]$ complexes in solution (An = Th, U, Np, Pu) are provided in reference [28]. Best-fit parameters are displayed in Table 1 together with the $[An(nta)_2]$ fit parameters. The acti-

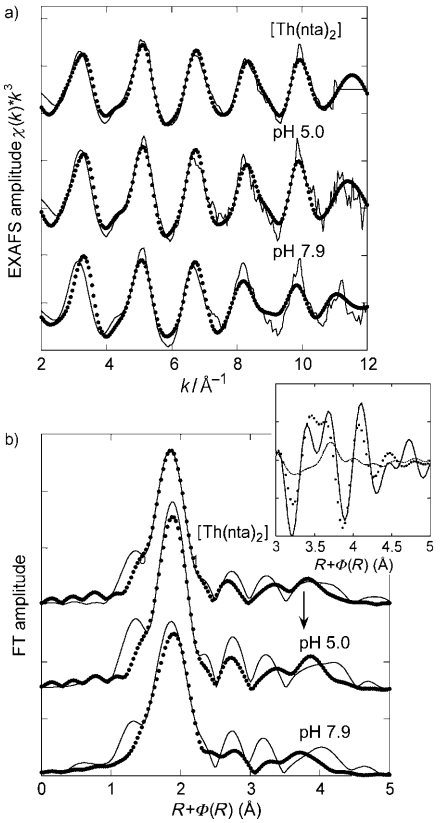

Figure 3. a) Experimentally measured (straight line) and adjusted (dots) EXAFS oscillations at the thorium L_{III} edge of $[Th(nta)_2]$ complex and Th–NTA–Tf at pH 5.0 and 7.9. b) Corresponding experimentally measured (straight line) and adjusted (dots) Fourier transformations. Insert: Imaginary part of the Fourier transform of the spectrum of $[Th(nta)_2]$. Straight line = experimental, dots = fit with triple scattering contributions, dash line = fit without triple scattering contributions.

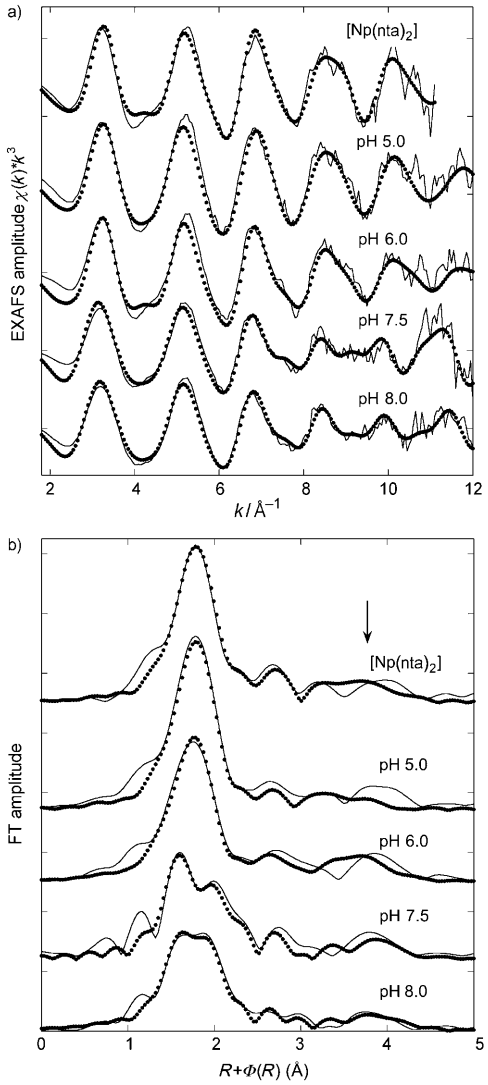

Figure 4. a) Experimentally measured (straight line) and adjusted (dots) EXAFS oscillations at the neptunium L_{III} edge of $[Np^{IV}(nta)_2]$ complex and Np^{IV}–NTA–Tf at pH values from 5.0 to 8.0. b) Corresponding experimentally measured (straight line) and adjusted (dots) Fourier transformations.

nidic contraction is clearly visible, with $\Delta d \sim 0.09$ Å between Th^{IV} and Pu^{IV}. For all these samples, the difference between the adjusted distances and the distances in the corresponding $[An^{IV}(nta)_2]$ complex were within the range of EXAFS uncertainty (± 0.02 Å). This is consistent with the assessment that Th^{IV} remains in the form of $[Th^{IV}(nta)_2]$ whatever the pH, and that the same is the case with Np^{IV} and Pu^{IV} when the pH is lower than 7. Around $R+\Phi = 3$ to 4 Å, the weak contributions corresponding to multiple scattering paths are a fingerprint of the outer shell carbon and distal oxygen atoms of NTA {six of them for $[An(nta)_2]$}. The insert of Figure 3b shows the improvement of the fit (imaginary part of the FT) in this region achieved by including these contributions as described in the Experimental Section. Nevertheless, fitting of this region remains difficult for some spectra (Th at pH 7.9, for instance) and may be complicated by the concomitant presence of contamination by hydrolysed products (see below).

From the spectrophotometric and gammametric data, we may recall that at pH $\geq$7.5, Np^{IV} is quantitatively complexed with transferrin. The similarity between Np^{IV} and Pu^{IV} EXAFS spectra at pH $\geq$7.5 discussed above suggests that Pu^{IV} is also complexed by the protein. Moreover, attempts to fit these data as $[An(nta)_2]$ complexes led to unrealistic distortions of the distances. As a result, a new fitting model based on a Ce^{IV}–NTA–Tf cluster was used, as described in the Experimental Section. Two oxygen contributions, two shells of carbon atoms, and one shell of triple scattering path from the NTA anion were necessary to adjust the EXAFS An–NTA–Tf spectra at pH >7.5 (An = Np and Pu, pH 7.5 and 8). Best-fit parameters are displayed in Table 2. These results show that for both cations, and whatever the pH, the fitted distances are comparable within the range of EXAFS uncertainty. This suggests that once formed, the An–NTA–Tf complexes (An = Np, Pu) are stable up to pH 8.0, confirming the gammametric data for neptunium. Two additional carbon contributions were found to be necessary in order to obtain a reasonable fit. However,

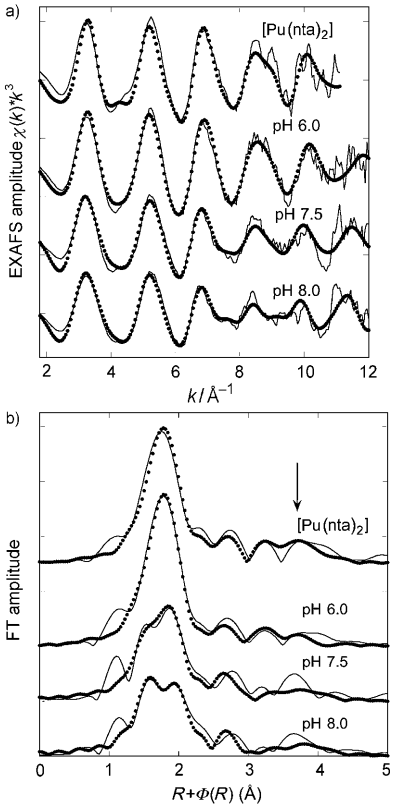

Figure 5. a) Experimentally measured (straight line) and adjusted (dots) EXAFS oscillations at the plutonium L_{III} edge of $[Pu^{IV}(nta)_2]$ complex and Pu^{IV}–NTA–Tf at pH values from 6.0 to 8.0. b) Corresponding experimentally measured (straight line) and adjusted (dots) Fourier transformations.

Table 1. Best-fit parameters of the EXAFS $[An(nta)_2]$ and An-NTA–Tf spectra at pH <7 (An = Th^{IV}, Np^{IV} and Pu^{IV}), fitted as described in reference [37].[a]

Sample	Neighbors [Å]	S_0^2, e_0 [eV] R factor ε, $\Delta\chi^2_v$
Th^{IV}–NTA[b]	6 O at 2.41(1), $\sigma^2=0.0050$	1.1
	2 N at *2.77*, $\sigma^2=0.0121$	7.4 eV
	6 C at *3.37*, $\sigma^2=0.0091$	4.6 %; 0.0036; 0.3
	6 C at *3.52*, $\sigma^2=$*0.0091*	
Th–NTA–Tf-5.0	6 O at 2.42(1), $\sigma^2=0.0051$	1.2
	2 N at *2.77*, $\sigma^2=0.0246$	8.8 eV
	6 C at *3.38*, $\sigma^2=0.0078$	6.9 %; 0.0058; 0.2
	6 C at *3.53*, $\sigma^2=$*0.0078*	
Th–NTA–Tf-7.9	6 O at 2.43(1), $\sigma^2=0.0057$	1.1
	2 N at *2.79*, $\sigma^2=0.0127$	7.1 eV
	6 C at *3.39*, $\sigma^2=0.0055$	7.6 %; 0.0014; 4.0
	6 C at *3.56*, $\sigma^2=$*0.0055*	
Np^{IV}–NTA[b]	6 O at 2.34(1), $\sigma^2=0.0070$	1.1
	2 N at *2.69*, $\sigma^2=0.0175$	4.5 eV
	6 C at *3.31*, $\sigma^2=0.0131$	3.2 %; 0.0044; 0.1
	6 C at *3.45*, $\sigma^2=$*0.0131*	
Np–NTA–Tf-5.0	6 O at 2.34(1), $\sigma^2=0.0069$	1.2
	2 N at *2.67*, $\sigma^2=0.0312$	3.9 eV
	6 C at *3.30*, $\sigma^2=0.0228$	3.0 %; 0.0035; 0.3
	6 C at *3.44*, $\sigma^2=$*0.0228*	
Np–NTA–Tf-6.0	6 O at 2.33(1), $\sigma^2=0.0086$	1.2
	2 N at *2.68*, $\sigma^2=0.0298$	3.7 eV
	6 C at *3.30*, $\sigma^2=0.0159$	3.5 %; 0.0025; 0.4
	6 C at *3.44*, $\sigma^2=$*0.0159*	
Pu^{IV}–NTA[b]	6 O at 2.34(1), $\sigma^2=0.0096$	1.4
	2 N at *2.69*, $\sigma^2=0.0124$	3.6 eV
	6 C at *3.31*, $\sigma^2=0.0133$	4.0 %; 0.0056; 0.1
	6 C at *3.45*, $\sigma^2=$*0.0133*	
Pu–NTA–Tf-6.0	6 O at 2.33(1), $\sigma^2=0.0078$	1.3
	2 N at *2.68*, $\sigma^2=0.0422$	3.4 eV
	6 C at *3.31*, $\sigma^2=0.0189$	2.5 %; 0.0038; 0.1
	6 C at *3.44*, $\sigma^2=$*0.0189*	

[a] σ^2 (Å^2) is the Debye–Waller factor, S_0^2 is the global amplitude factor, e_0 (eV) is the energy shift factor, r and $\Delta\chi^2_v$ are the R factor and the quality factor of the fit in R space, respectively, and ε is the average noise of the spectrum in $k^3\chi(k)$. Uncertainties are given in brackets. Numbers in italics have been linked together. Numbers of neighbors have been fixed. [b] Values from reference [28].

as would be expected for very flexible organic ligands, the associated Debye–Waller factors are also very high, confirming that from the EXAFS point of view these atoms are very fuzzy. The presence of weak contributions around $R+\Phi=3$ to 4 Å (arrows in Figures 3b, 4b, 5b) has two possible origins. As described in the Experimental Section, triple scattering paths from carbon shells, and in particular from the distal oxygens of the NTA anion (three of them for An–NTA–Tf), were found to contribute to this region of the Fourier transform. Interestingly, for Th these contributions are of constant amplitude, whereas for Np and Pu they seem to decrease in intensity for spectra recorded at pH values higher than 7 (except for the spectrum of Pu pH 7.5, because of a strong glitch at 10.5 Å^{-1}), suggesting that fewer than two NTA anions are involved in the An–NTA–Tf complexes. How-

Table 2. Best-fit parameters of the EXAFS $[An(nta)_2]$ and An–NTA–Tf spectra at pH >7 (An = Th^{IV}, Np^{IV} and Pu^{IV}). σ^2 (Å^2) is the Debye–Waller factor, S_0^2 is the global amplitude factor, e_0 (eV) is the energy shift factor, r and $\Delta\chi^2_v$ are the R factor and the quality factor of the fit in R space, respectively, and ε is the average noise of the spectrum in $k^3\chi(k)$. Uncertainties are given in brackets. Numbers in italics have been linked together.

Sample	Neighbors [Å]	S_0^2,	e_0 [eV]	R factor	ε	$\Delta\chi^2_v$
Np–NTA–Tf-7.7	*3.9* O,N at 2.22(1), $\sigma^2=0.0022$	0.8	6.7	6.0	0.0013	1.2
	5.1 O,N at 2.39(1), $\sigma^2=0.0017$					
	3.9 C at 3.25(6), $\sigma^2=$*0.0091*					
	8.4 C at 3.41(3), $\sigma^2=$*0.0091*					
Np–NTA–Tf-8.0	*4.0* O,N at 2.23(1), $\sigma^2=0.0041$	0.8	7.6	3.2	0.0033	0.1
	5.0 O,N at 2.39(1), $\sigma^2=0.0026$					
	4.1 C at 3.27(3), $\sigma^2=$*0.0063*					
	6.5 C at 3.44(2), $\sigma^2=$*0.0063*					
Pu–NTA–Tf-7.7	*3.5* O,N at 2.21(1), $\sigma^2=0.0071$	0.8	7.7	7.5	00.0036	0.2
	5.5 O,N at 2.37(1), $\sigma^2=0.0047$					
	8.5 C at 3.33(3), $\sigma^2=$*0.0113*					
	4.7 C at 3.47(6), $\sigma^2=$*0.0113*					
Pu–NTA–Tf-8.0	*3.9* O,N at 2.21(1), $\sigma^2=0.0049$	0.8	8.1	7.1	0.0037	0.1
	5.1 O,N at 2.38(1), $\sigma^2=0.0033$					
	6.6 C at 3.34(3), $\sigma^2=$*0.0085*					
	3.8 C at 3.59(6), $\sigma^2=$*0.0085*					

ever, the fit quality in this region remains less satisfactory than might be expected. One of the reasons is the difficulty in evaluation of the structural distortion of the NTA distal oxygen atoms while the actinide cation is bound in the protein binding site. In addition, as mentioned previously, the concomitant presence of actinide hydrolysed products can never be totally excluded. The presence of a more intense contribution at $R+\Phi=3.7$ Å in the Fourier transforms of some of the An–NTA–Tf and $[An(nta)_2]$ spectra suggests the occurrence of contamination by hydrolysed products. Indeed, attempts to add an An–An contribution did lead to significant improvements of some of the spectra in the 3.7 Å region but not to the global *R* factor of the fit. However, the UV/Vis/NIR spectrophotometry and microfiltration data demonstrate that hydrolysed products remain negligible. Quantification of these in all the samples through the An–An contribution at $R+\Phi=3.7$ Å in the EXAFS data Fourier transforms is difficult given the limited accuracy of EXAFS with amplitude factors, as well as the presence of mix multiple scattering contributions in this region. The contribution of An−OH from hydrolysed products is in the 2.20–2.22 Å range for plutonium.[31,32] In all the EXAFS An–NTA–Tf sample spectra this contribution would overlap with the existing short-range distance and its presence could not therefore be tested. On the other hand, in all the EXAFS spectra of $[An(nta)_2]$ species, attempts to add a similar short-length contribution of this type lead to degradation of the *R* factor. If it is borne in mind that the $[An(nta)_2]$ and An–NTA–Tf samples all exhibit the same long-range $R+\Phi=3.7$ Å contribution, the absence of short-range contribution in the $[An(nta)_2]$ samples undoubtedly precludes major contamination of all the samples by hydrolysed products. In summary, one can rule out the formation solely of actinide hydrolysed products, rather than An–NTA–Tf complexes, although minor contamination must be present. The $R+\Phi=3$ to 4 Å regions are the results of complicated combinations of triple scattering paths originating from the NTA anions, other multiple scattering contributions from the transferrin itself that are difficult to estimate, and possible minor An–An contributions from hydrolysis contamination.

Discussion

A two-step reaction can be proposed for the complexation of actinides with transferrin. The first step of the reaction is the formation of the $[An(nta)_2]$, as described previously.[37] For the cation to be reachable by the protein, at least one molecule of NTA must leave the actinide coordination sphere. On the other hand, at least one NTA ligand is required as a synergetic anion for complexation to occur. Accordingly, and with no consideration of thermodynamic or kinetic constants, combination of all the above data suggests that the second step must be as follows:

$$2[An^{IV}(nta)_2] + ApoTf \overset{pH>7}{\rightleftharpoons} [(An^{IV}nta)_2Tf] + 2NTA \qquad (1)$$

With neptunium and plutonium, Equation (1) is valid from pH 7.5 to pH 8.0, above which precipitation of the actinide hydroxide occurs. For thorium, Equation (1) was not observed, whatever the spectroscopic technique and for all the given pH values. These results contrast with previous literature data in suggesting that Th^{IV} complexation with transferrin occurs at $6 < pH < 9.5$ even in the presence of excess NTA at pH 7.2.[17]

Several tentative explanations may be invoked, although the precise mechanism driving actinide chelation by *apo*Tf is not known at this point. The N-terminal site, for instance, seems to be slightly smaller than the C-terminal site and cannot readily accommodate cations larger than Eu^{III}.[4] This may explain why Th^{IV}, which has the largest ionic radius of the series, is not accommodated by the N-terminal site ($r_i^{Eu^{III},CN=8} = 120$ Å $\sim r_i^{Th^{IV},CN=8} = 119$ Å $\gg r_i^{Np^{IV},CN=8} = 112$ Å $> r_i^{Pu^{IV},CN=8} = 110$ Å). However no conclusion for the C-terminal site can be drawn. By this simplistic size criterion, Th^{IV} may be the worst actinide candidate to enter the transferrin complexation sites. In view of the biological similarities between Fe^{III} and Pu^{IV},[8] one can assume that behavior with regard to hydrolysis may be an important parameter for transferrin uptake. Indeed, thorium(IV) has the weakest hydrolysis constant of the series: $\log\beta_{11-Th^{IV}} \approx 11.5 < \log\beta_{11-Np^{IV}} \approx 14.5 < \log\beta_{11-Pu^{IV}} \approx 14.5$.[33]

When complexation of Np^{IV} and Pu^{IV} occurs, the An–O distance in the first oxygen shell is 0.12 Å shorter than the Np–O distance in $[Np^{IV}(nta)_2]$ and the Pu–O distance in $[Pu^{IV}(nta)_2]$. Many crystallographic structures of transferrin complexes demonstrate that the tyrosine–cation distance is much shorter than the distance between the cation and the other amino acids at the transferrin complexation site (i.e., aspartate and histidine). In human holotransferrin (PDB reference: 1B3E[34]), for example, the mean Fe–tyrosine distance is 1.90 Å whereas the mean Fe–aspartate, –histidine and –carbonate distance is 2.04 Å. The difference between these two characteristic distances—$\Delta d_{Fe-O}=0.14$ Å—is comparable to $\Delta d_{Np,Pu-O}=0.12$ Å. The splitting of the first shell of neptunium/plutonium described by the EXAFS data analysis may therefore be attributed to cation complexation through at least one tyrosine at the protein complexation site. Unfortunately, the recorded EXAFS data do not allow us to distinguish the carbon atoms of the tyrosine rings from the other carbon atoms. The UV spectrophotometric signature of the phenolate–metal bond[10] at 240 nm could not be observed either, because of the spectrophotometer cut-off in glove-box configuration. Another assumption is that such short distances could also be attributable to several hydroxo bonds, typical Pu−OH bond lengths being of the order of 2.20–2.22 Å.[31,32] Formation of this type of bond is not unexpected given the high pH of the media and the strong tendency of actinides to undergo hydrolysis. As mentioned before, one may rule out the occurrence of hydrolysed products as the sole explanation for the short An–O distance, but a mixed complex is possible.

Interestingly, the number of oxygen atoms in the first contribution (three or four) is higher than the number of tyro-

sine residues at the transferrin complexation site (two). Consequently, we propose the formation of a mixed hydroxo–transferrin complex in which actinides are bound with transferrin through at least one tyrosine residue, both An–tyrosine and An−OH bonds having comparable lengths.

The structural role of NTA in the protein complexation site is also not fully characterized. However NTA is often described as a synergistic anion. Its participation in the Np/Pu coordination sphere at the transferrin binding site is indeed suggested by the presence of a long-range contribution (arrows in Figure 3b, Figure 4b, and Figure 5b) in the Fourier transformed spectra, even at pH values higher than 7, although the concomitant presence of possible hydrolysed products and additional multiple scattering contributions complicates the analysis. Because actinide(IV) cations accommodate large coordination numbers (typically between eight and 10) one can assume that an additional ligand is needed to complete the actinide polyhedron. In comparison, Fe^{III} is linked to four ligands from the protein binding site plus two from the synergistic carbonate anion. NTA is also known to bind Fe^{III} in a mixed Tf–NTA complex.[35] From these qualitative considerations one can assume that one NTA ligand participates in the cation polyhedron at the protein binding site. It is planned in the future to undertake ^{13}N NMR with marked ^{13}NTA to provide better understanding of the role of the aminocarboxylic acid.

Finally, comparison of our results with available data on holotransferrin suggests some similarities between the behavior of Fe^{III} and Np^{IV}/Pu^{IV}.

1) We have shown here the influence of pH on Np^{IV} complexation with transferrin. Np^{IV} is not complexed at pH <7, and the complexation can be considered as quantitative at pH ~7.4. This pH effect is consistent with the in vivo transferrin "cycle". Indeed, iron in blood is complexed at pH ~7.4 and is released in the cell when the proton pump increases acidity at pH ~5 in the vesicle in which transferrin is internalized.
2) Np^{IV} and Pu^{IV} appear to be quantitatively bound by *apo*Tf.
3) It was assumed in this work that the iron complexation site is the actinide bonding site, as reported for Pu^{IV}.[36] This means that at least one tyrosine residue could participate in the actinide coordination sphere (we recall that two tyrosine residues are involved for iron complexation) forming a mixed hydroxo–transferrin complex in which actinides are bound with transferrin both through An–tyrosine and through An−OH bonds.

Conclusions

As shown by physiological studies from the abundant literature, actinides in plasma are assumed to be mainly complexed to transferrin, the iron carrier protein. This work sheds light on the uptake of thorium(IV), neptunium(IV), and plutonium(IV), in comparison with Fe^{III}, by *apo*Tf. It provides new structural data on the actinide complexation site inside the protein. First of all, we observed that the behavior of Th^{IV} differs from that of the two parent actinide cations neptunium and plutonium. According to our data, thorium is not bound to transferrin under our experimental conditions. For neptunium and plutonium, the pH dependence of transferrin uptake was demonstrated with the aid of a combination of spectroscopic and gammametric techniques. Complexation is at its maximum at a pH close to physiological value, whereas below pH 7 the two actinide cations remain in the $[An(nta)_2]$ form. Furthermore, EXAFS measurements at the actinide L_3 edges were used to describe the actinide coordination spheres: a short oxygen contribution attributed to a combination of tyrosine residues and hydroxo bonds, a long oxygen contribution belonging to the other residues of the transferrin complexation site, as well as the remaining NTA synergistic ligand. Although the precise mechanisms that drive actinide uptake by transferrin have not yet been fully elucidated, these data suggest that subtle differences in physical chemical properties, as between thorium, neptunium and plutonium at oxidation state +IV, may lead to significant differences in behavior with regard to their interaction with transferrin. From a physiological point of view, these results are of major consequence. From a more fundamental chemical point of view, they address the question of fine-tuning of actinide reactivity across the series when specific intricate ligands, such as transferrin (in a simplistic scheme), are involved.

Experimental Section

Actinide stock solutions: Actinide starting materials were obtained from the CEA inventory. Actinides are radioactive elements and were all handled in dedicated glove boxes. Plutonium (^{239}Pu) and neptunium (^{237}Np) were purified by ion exchange on an anionic resin (AGMP1, DOWEX). The stock solution of Np^{IV} ([Np] = 50 mM) was prepared by means of a hydroxyammonium chloride (250 mM) reduction (70 °C) of a Np^{V} solution obtained by dissolving $Np^{V}O_2OH{\cdot}xH_2O$ ($x \approx 2.5$) in hydrochloric acid (≈1 M). The reaction was monitored by spectrophotometry in order to control neptunium concentration, and to ensure that less than 1% Np^{V} remained in the solution. The stock solution of Pu^{IV} ([Pu] = 32 mM) was prepared in nitric acidic solution (0.55 M). Solid thorium nitrate $Th(NO_3)_4{\cdot}5H_2O$ (Prolabo) was used without further purification. The stock solution of Th^{IV} ([Th] = 20 mM) was obtained by dissolving thorium nitrate in a hydrochloric acid solution (0.1 M).

Apotransferrin (*apo*Tf): This was a human protein used as provided (Sigma–Aldrich, purity >96%).

An^{IV}–apotransferrin complexes (An = Th, Np, Pu): All samples were prepared in water in the presence of the acid–base buffer *N*-(2-hydroxyethyl)piperazine-*N*′-(2-ethanesulfonic acid) (HEPES, provided by Sigma–Aldrich).

The actinides were first protected from hydrolysis by use of nitrilotriacetic acid (NTA, used as provided, Sigma–Aldrich) as a complexing agent, under physiological conditions (pH 7.4). NTA has also been reported as act as a synergistic anion,[4] so it would be expected to protect the actinide but also to allow its complexation with transferrin. The $[An(nta)_2]$ complexes (An = Th, Np, Pu), which have been reported in solid state and in solution,[37] are stable at pH values of around 6.5, the pH zone of stability for transferrin being between 5 and 8.

An^{IV}–NTA complexes were prepared by addition of the An^{IV} stock solution to a solution of a stoichiometric quantity (1:2) of NTA in water with HEPES. The An/NTA solution was diluted in water with HEPES, and the pH was adjusted with small amounts of LiOH (1 M in water, the pH was monitored with 0.2 unit pH paper, pH range: 5–8). Freeze-dried apotransferrin was then carefully weighed and solubilized in the An/NTA solution. Measurements were made several minutes after preparation for laboratory techniques and two days after preparation for synchrotron experiments.

Note that actinide manipulation requires working inside a glovebox, which considerably hinders techniques used for protein preparations and handling.

Table 3 summarizes all the sample compositions.

Table 3. Sample compositions for the synthesis of An–NTA–Tf (An = Th^{IV}, Np^{IV}, Pu^{IV}) complexes. EXAFS = extended X-ray absorption fine structure, UV = UV/Visible spectrophotometry, UF = ultrafiltration/gammametry.

Sample	Exp. techniques	An/NTA/Tf ratio	pH
$[Th(nta)_2]$	EXAFS[37]+UF	1:2:0	6–7
$[Np(nta)_2]$	EXAFS[37]+UV+UF	1:2:0	6–7
$[Pu(nta)_2]$	EXAFS[37]	1:2:0	6–7
Th–NTA–Tf-5.0	EXAFS	1:2:0.5	5.0
Th–NTA–Tf-6.5	UF	1:2:0.5	6.5
Th–NTA–Tf-7.4	UF	1:2:0.5	7.4
Th–NTA–Tf-7.9	UF+EXAFS	1:2:0.5	7.9
Np–NTA–Tf-5.0	UF+EXAFS	1:2:0.5	5.0
Np–NTA–Tf-6.0	UF+EXAFS	1:2:0.5	6.0
Np–NTA–Tf-7.2	UF	1:2:0.5	7.2
Np–NTA–Tf-7.5	UF+EXAFS	1:2:0.5	7.5[a]
Np–NTA–Tf-8.0	UF+EXAFS	1:2:0.5	8.0
Pu–NTA–Tf-6.0	EXAFS	1:2:0.5	6.0
Pu–NTA–Tf-7.5	EXAFS	1:2:0.5	7.5
Pu–NTA–Tf-8.0	EXAFS	1:2:0.5	8.0

[a] 7.7 for EXAFS.

UV/Visible/NIR spectrophotometry: Measurements were carried out with a Shimadzu 3101 spectrophotometer at room temperature, with a 0.1 cm path-length quartz cell. The scanning interval was fixed at 1 nm, with a slit width of 0.8 nm, from 300 nm to 1200 nm for the actinide samples, and from 250 nm to 650 nm for non-radioactive samples.

Microfiltration: Microfiltration experiments were undertaken with Microcon filters with a molecular weight cut-off of about 10 kDa. Centrifugation was performed with a Minispin plus Eppendorf centrifuge. The molecular weight cut-off was chosen in such a way that transferrin adducts were retained on the filter ($M_W > 75$ kDa), whereas cations not bound to transferrin (such as $[An^{IV}(nta)_2]$ complexes, $M_W \in [619;632]$ g mol^{-1}) were not retained. However, it should be noted that the separation of actinide–transferrin complexes from colloidal species (which according to Moriyama et al.[38] can have molecular weights higher than 100 kDa) is not possible.

The sample solution (200 μL) was deposited on a Microcon filter and was then centrifuged for 30 min (9600 g). The filter was rinsed three times with an aqueous HEPES solution adjusted to the sample pH, with the same centrifugation conditions being maintained ([HEPES] = 0.5 M).

Gamma spectrometry: Measurements were carried out with a Canberra Eurisys gamma spectrometer fitted with a germanium crystal. The γ spectrometer was calibrated with a multi-γ standard containing ^{60}Co, ^{105}Cd, ^{137}Cs, and ^{241}Am (LEA, Laboratoire Etalons d'Activité). The filtrate solution (500 μL) was transferred to a double-walled vial for radioactive samples and placed on the detector with a wedge ensuring detector with a wedge, ensuring that the geometry remained the same for all the samples. Np samples were measured for 2 h (^{237}Np specific activity = 26×10^6 Bq g^{-1}) and Th samples for 48 h (^{232}Th specific activity = 4100 Bq g^{-1}). Uncertainties were taken into account by considering the errors in sample preparation (dilution, weighing, geometrical factors) and the statistical error in gamma counting. Accordingly, uncertainties were estimated to be around 10% for neptunium and 15% for thorium.

EXAFS data acquisition, processing and analysis

Data acquisition and processing: EXAFS spectra were recorded at the European Synchrotron Radiation Facility (ESRF, ring operated at 6 GeV with 200 mA).

Thorium, neptunium, and plutonium L_{III}-edge EXAFS spectra were recorded at the ESRF Rossendorf beam line (BM20). BM20 is equipped with a water-cooled double-crystal Si(111) monochromator. Higher harmonics were rejected by use of two collimating Pt coated mirrors. A 13-element Ge solid-state detector was used for data collection in fluorescence mode. Monochromator energy calibration of the absorption spectra was carried out at the yttrium K-edge (17052 eV at the absorption maximum). All measurements were recorded in double-layered 200 μL cells specifically designed for radioactive samples, at room temperature.

Data were processed by use of the Athena code.[39] Background removal was performed by use of a pre-edge linear function. Atomic absorption was simulated with a cubic spline function.

Data fitting: The extracted EXAFS signal was fitted in *R* space without any additional filtering by use of the ARTEMIS code.[39] All adjustments were made in the *R* space. The *R* factor and quality factor ($\Delta\chi^2_v$) are both provided as an indication of fit quality in the *R* space, whereas the average noise of the spectrum (ε) was estimated by back-Fourier transformation in $k^3\chi(k)$ mode above 6 Å with the Cherokee code.[40]

In all the fits, only one global amplitude factor and one energy threshold factor were considered for all the contributions.

Kaiser windows with $k \in [2.0\ Å^{-1}; 11.0/12.0\ Å^{-1}]$ and fitting range with $R \in [1.0\ Å; 5.0\ Å]$ were used.

Th–NTA–Tf at all pH values and Np–NTA–Tf and Pu–NTA–Tf at pH < 7: Phases and amplitudes were calculated by use of the Feff82 code from a calculated $[An^{IV}(nta)_2(H_2O)_{0.1}]$ cluster.[37] Spectra were fitted as previously described for the first coordination sphere.[37] In addition, three shells of carbon atoms in the triple-scattering approximation (An-$C_{carboxy}$-O, An-C_{alphaN}-N, and An-$C_{carboxy}$-O_{distal}) were included in the fitting procedure in a semi-rigid model. Debye–Waller factors for the An-C_{alphaN}-N and An-$C_{carboxy}$-O triple scattering paths were found to be highly correlated and often unstable. In such cases they were set to the average reasonable value. The Debye–Waller factor of the An-$C_{carboxy}$-O_{distal} path was found meaningful and always equal to about 0.0150 Å^2. This path contributes mostly to the contribution at $R+\Phi \approx 3.7$ Å as discussed in the main text. The instability of the fits in this regions comes from the complicated path interference that arises from the outer-shell carbon atoms of the NTA molecule.

Np–NTA–Tf and Pu–NTA–Tf at pH > 7: Phases and amplitudes were calculated by Feff82 code from a Ce^{IV}–NTA–Tf cluster obtained from quantum chemical calculations, derived from the crystallographic structure of Ce^{IV}–Tf (PDB reference: 1FCK).[41] In this structure, only ligands directly coordinated to the cation were kept out of the amino acid residues (two tyrosines, one histidine, one aspartic acid), and one molecule of NTA was added in the actinide coordination sphere, linked by three oxygen and one nitrogen atoms, in accordance with the known An^{IV}–NTA structure.[37] Two oxygen contributions, two shells of carbon atoms in the single-scattering approximation, and one carbon shell An-$C_{carboxy-NTA}$-O in the triple-scattering paths were used. This path originates from the assumed remaining NTA in the metal binding site of the protein (see discussion above). The numbers of oxygen atoms from the two first shell contributions were linked together, totaling nine. The number of carbon atoms was fitted freely, with the same Debye–Waller factor for all the carbon shells used in the fit.

Both complexation sites of transferrin were considered to be equivalent with respect to EXAFS sensitivity.

Acknowledgements

This work was supported by the French Environmental Toxicology Program and CEA/DEN/DDIN/MR. XAS measurements were carried out at ESRF, a European user facility, on beam line ROBL (BM20).

[1] D. M. Taylor, *J. Alloys Compd.* **1998**, *271*, 6.
[2] P. W. Durbin, Actinides in *The Chemistry of the Actinide and Transactinide Elements*, 3rd ed. (Eds.: L. R. Morss, N. M. Edelstein, J. Fuger), Springer, Heidelberg, **2006**, p. 3339.
[3] A. Jeanson, C. Den Auwer, P. Moisy, C. Vidaud in *Speciation Techniques and Facilities for Radioactive Materials at Synchrotron Light Sources* (Proceeding of the workshop Actinide-XAS 2006, Karlsruhe), OECD **2007**, p. 235.
[4] E. N. Baker, *Adv. Inorg. Chem.* **1994**, *41*, 389.
[5] P. Aisen, A. Leibam, J. Zweier, *J. Biol. Chem.* **1978**, *253*, 1930.
[6] J.-N. Octave, Y.-J. Schneider, A. Trouet, R. R. Crichton, *Trends Biochem. Sci.* **1983**, *8*, 217.
[7] M. R. Schlabach, G. W. Bates, *J. Biol. Chem.* **1975**, *250*, 2182.
[8] K. N. Raymond, W. L. Smith, F. L. Weitl, P. W. Durbin, E. S. Jones, K. Abu-Dari, S. R. Sofen, S. R. Cooper in *Lanthanide and Actinide Chemistry and Spectroscopy* (Ed.: N. M. Edelstein), ACS, Washington, **1980**, p. 143.
[9] H. Li, P. J. Sadler, H. Sun, *Eur. J. Biochem.* **1996**, *242*, 387.
[10] W. R. Harris, *Struct. Bonding (Berlin)* **1998**, *92*, 121.
[11] R. Racine, PhD thesis, Université Paris XI Orsay (France), **2001**.
[12] D. S. Popplewell, G. Boocock in *Diagnosis and Treatment of Deposited Radionucleides* (Eds.: H. A. Kornberg, W. D. Norwood), Excerpta Medica Foundation, Richland, **1968**, p. 45.
[13] B. J. Stover, F. W. Bruenger, W. Stevens, *Radiat. Res.* **1968**, *33*, 381.
[14] E. Peter, M. Lehmann, *Int. J. Radiat. Biol.* **1981**, *40*, 445.
[15] R. Wirth, D. M. Taylor, J. Duffield, *Int. J. Nucl. Med. Biol.* **1985**, *12*, 327.
[16] F. W. Bruenger, D. R. Atherton, W. Stevens, B. J. Stover in *Research in Radiobiology, Annual report*, University of Utah College of Medicine, **1971**, p. 212.
[17] W. R. Harris, C. J. Carrano, V. L. Pecoraro, K. N. Raymond, *J. Am. Chem. Soc.* **1981**, *103*, 2231.
[18] C. Vidaud, S. Gourion-Arsiquaud, F. Rollin-Genetet, C. Torne-Celer, S. Plantevin, O. Pible, C. Berthomieu, E. Quéméneur, *Biochemistry* **2007**, *46*, 2215.
[19] W. Stevens, F. W. Bruenger, D. R. Atherton, J. M. Smith, G. N. Taylor in *Proceedings of the Snowbird Actinide Workshop* (Ed.: M. E. Wrenn), RD Press, Salt Lake City, **1979**, p. 457.
[20] J. R. Cooper, G. N. Stradling, H. Smith, S. E. Ham, *Int. J. Radiat. Biol.* **1982**, *41*, 421.
[21] S. Scapolan, PhD thesis, Université Paris XI Orsay (France), **1998**.
[22] I. Llorens, C. Den Auwer, P. Moisy, E. Ansoborlo, C. Vidaud, H. Funke, *FEBS J.* **2005**, *272*, 1739.
[23] C. Den Auwer, I. Llorens, P. Moisy, C. Vidaud, F. Goudard, C. Barbot, P. L. Solari, H. Funke, *Radiochim. Acta* **2005**, *93*, 699.
[24] G. Grossmann, M. Neu, E. Pantos, F. J. Schwab, R. W. Evans, E. Townes-Andrews, P. F. Lindley, H. Appel, W.-D. Thies, S. S. Hasnain, *J. Mol. Biol.* **1992**, *225*, 811.
[25] J. R. Duffield, D. M. Taylor, *Inorg. Chim. Acta* **1987**, *140*, 365.
[26] J. Duffield, D. M. Taylor, S. A. Proctor, *Int. J. Nucl. Med. Biol.* **1986**, *12*, 483.
[27] D. M. Taylor, A. Seidel, F. Planas-Bohne, U. Schuppler, M. Neu-Müller, R. Wirth, *Inorg. Chim. Acta* **1987**, *140*, 361.
[28] A. B. Yusov, A. M. Fedoseev, *Radiochemistry* **2003**, *45*, 339.
[29] H. Moriyama, M. I. Pratopo, K. Higashi, *Sci. Total Environ.* **1989**, *83*, 227.
[30] E. A. Hudson, J. J. Rehr, J. J. Bucher, *Phys. Rev. B* **1995**, *52*, 13815.
[31] J. Rothe, C. Walther, M. A. Denecke, T. Fanghänel, *Inorg. Chem.* **2004**, *43*, 4708.
[32] S. D. Conradson, *Appl. Spectrosc.* **1998**, *52*, 252A.
[33] V. Neck, J. I. Kim, *Radiochim. Acta* **2001**, *89*, 1.
[34] M. C. Bewley, B. M. Tam, J. Grewal, S. He, S. Shewry, M. E. P. Murphy, A. B. Mason, R. C. Woodworth, E. N. Baker, R. T. A. Macgillivray, *Biochemistry* **1999**, *38*, 2535.
[35] K. Mizutani, H. Yamashita, H. Kurokawa, B. Mikami, M. Hirose, *J. Biol. Chem.* **1999**, *274*, 10190.
[36] G. Grossmann, M. Neu, E. Pantos, F. J. Schwab, R. W. Evans, E. Townes-Andrews, P. F. Lindley, H. Appel, W.-D. Thies, S. S. Hasnain, *J. Mol. Biol.* **1992**, *225*, 811.
[37] L. Bonin, D. Guillaumont, A. Jeanson, C. Den Auwer, M. Grigoriev, J-C. Berthet, C. Hennig, A. Scheinost, P. Moisy, *Inorg. Chem.* **2009**, *48*, 3943 .
[38] H. Moriyama, M. I. Pratopo, K. Higashi, *Sci. Total Environ.* **1989**, *83*, 227.
[39] B. Ravel, M. Newville, *J. Synchrotron Radiat.* **2005**, *12*, 537.
[40] A. Michalowicz, EXAFS code, to be found under http://www.icmpe.cnrs.fr.
[41] H. M. Baker, C. J. Baker, C. A. Smith, E. N. Baker, *J. Biol. Inorg. Chem.* **2000**, *5*, 692.

Received: May 7, 2009
Revised: August 31, 2009
Published online: November 30, 2009

